Molecular Dynamics of Self-Assembled Monolayer Formation in Soft Nanolithgoraphy

D. Heo[*], M. Yang[*], and J. Jang[**]

[*]Department of Chemistry, Chungbuk National University, Cheongju 361-763, Korea
[**]Department of Nanomaterials Engineering, Pusan National University, Miryang 627-706, Korea, jkjang@pusan.ac.kr

ABSTRACT

Molecular dynamics simulation is performed to study the growth mechanism of self-assembled monolayer in the AFM tip-assisted soft nanolithography such as in dip-pen nanolithography. We investigate how the droplet created around the tip spreads out to become a monolayer on the substrate. The previous diffusion model assumes that molecules diffuse on top of molecules already adsorbed on the substrate. In contrast, our molecular simulation shows that a molecule on top pushes out a molecule below it and the molecule just pushed out in turn pushes out a molecule next to it. The monolayer grows through such a serial pushing. The present large scale (40 nm diameter) simulation reveals new features. For a relatively weak adsorbate-substrate binding, the monolayer has irregular branches. As the adsorbate-substrate binding strengthens, the monolayer becomes compact, and reflects the rotational symmetry of substrate. A substrate with a hexagonal symmetry results in a hexagonal monolayer. An extremely strong molecule-substrate binding removes such an effect of the substrate anisotropy, giving rise to a circular monolayer. The monolayer periphery shows an initial diffusional growth in its time dependence followed by a slow expansion. The rates of self-assembled monolayer growth exhibit a turn-over behavior with increase in the attractive force between the adsorbate and substrate.

Keywords: dip-pen nanolithography, molecular dynamics simulation, monolayer, growth dynamics

1 INTRODUCTION

An atomic force microscope (AFM) tip serves as a useful tool for the deposition of monolayer on various substrates [1]. Due to its sharp asperity, this nanoscale tip serves as a point source of molecules which are usually designed to bind to a substrate. Currently, we poorly understand the mechanism of the monolayer growth at the molecular level. Due to the continuous downward flow of molecules from the tip, a droplet forms around the tip. This multilayered droplet subsequently spreads out to form a monolayer. As molecules in the upper layers step down to the substrate, the monolayer periphery broadens on the substrate. Exactly how this growth occurs? Elucidating this point will advance our understanding of the monolayer growth utilizing a nanoscale tip.

In our prior molecular dynamics (MD) simulation [2], we found that a molecule in the upper layer pushes a molecule below it out of its place, and the molecule just pushed out in turn pushes molecules next to it, and so on. Our MD however has been performed for a small-sized monolayer with a diameter of about 9 nm. Hence, it is not clear whether the above pushing mechanism should hold for a large monolayer. Herein, we investigate the growth dynamics of monolayer with a size comparable to typical dip-pen nanolithography experiments. For monolayer diameters up to 24 nm, we run MD simulations with trajectory lengths up to 1.5 ns. We investigate whether a novel mechanism emerges for such a large monolayer. We study how the monolayer shape depends on the molecule-substrate binding energy by systematically varying this energy in simulation.

2 SIMULATION DETAILS

We consider the deposition of a nonpolar, spherical molecule on gold (111) substrate. The molecular mass is set identical to that of 1-octadecanethiol ($CH_3(CH_2)_{17}SH$, ODT). We have also performed a simulation that explicitly takes into account the alkyl chain of ODT (by using a united atom model), and such a realistic simulation agrees with our coarse grained simulation.

The AFM tip is modeled as a hemisphere made of silicon atoms and ODT molecules are coated on the surface of the tip [figure 1]. The every interaction (molecule-molecule, molecule-tip atom, and molecule-gold atom interactions) is assumed to be a pairwise Lennard-Jones (LJ) potential [3], $U(r) = 4\varepsilon\left[\left(\sigma/r\right)^{12} - \left(\sigma/r\right)^{6}\right]$. LJ parameters, ε and σ, for the tip atom (silicon) and molecule are 0.4184 kJ/mol and 0.4 nm [4] and 5.24 kJ/mol and 0.497 nm, respectively. ε of our molecule is taken from that of stearic acid ethyl ester which is similar to ODT in mass. σ (= 0.497 nm) of our molecule is chosen to reproduce the experimental structure of the ODT monolayer on Au (111). σ for gold is 0.2655 nm [7] but ε value for gold has been systematically varied in order to examine the effects of molecule-substrate binding energy. The Lorentz-Berthelot combination rule [3] has been used for the interactions between unlike atomic or molecular species. The dissociation energy of ODT and

NSTI-Nanotech 2008, www.nsti.org, ISBN 978-1-4200-8503-7 Vol. 1

gold has been estimated as 3.182 kcal/mol [8]. We have set the lowest value of ε for molecule-substrate interaction as 3.182 kcal/mol. To inspect the effects of the molecule-substrate binding strength, we have considered additional values of ε.

The radius our hemispherical tip is 3.4 nm. Before starting the simulation of molecular deposition, we coat 2097 molecules on the tip by running a separate MD simulation. To do so, we positioned the molecules at the cubic lattice points near the tip. Then we artificially increased ε of tip 100 times its original value and ran MD simulation for 300 ps. Because of the artificially strong tip attraction, molecules spontaneously stick to the tip surface. The coated tip is used as the initial condition of MD [figure 1].

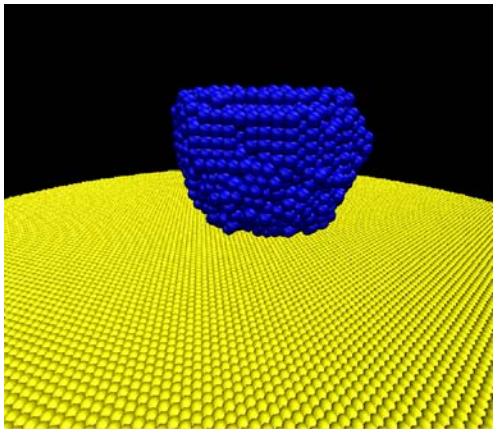

Figure 1: The initial configuration of molecular dynamics simulation. Total of 2097 molecules are coated on a spherical tip (made of 914 silicon atoms) above Au (111) surface (a single layer consisting of 17503 atoms).

The total number of molecules is 2097. The vertical distance from the tip end to the substrate is 1.3 nm. We include only a single layer of Au (111) substrate in simulation. The horizontal boundary of the gold substrate is a circle with a lateral diameter of 80 nm, and the substrate consists of 17503 gold atoms. The tip and gold atoms are frozen during simulation but they interact with molecules through LJ potentials. We propagated the molecular trajectory by using the velocity Verlet algorithm [3]. We used a time step of 3 fs, and the total time length of simulation was 1.5 ns. The temperature of our system was fixed to 300 K by using the themostat proposed by Berendsen et al. [9]

3 RESULTS

In all the cases, we found the pushing mechanism described in the Introduction prevails. We observed molecules sitting on top of other molecules for short times, but such molecules soon pushed molecules below to make their ways down to the substrate. No molecule stayed long enough on top and made it to the periphery to hop down to the substrate. The above pushing mechanism persisted even for a monolayer as large as 24 nm in diameter and for the strongest molecule-substrate binding energy considered in this work.

In figure 2, we present the final (t=1.5 ns) MD snapshot of the monolayer (top view) for four different molecule-substrate binding strengths. The tip is not drawn for visual clarity. For a relatively weak molecule-substrate binding (figure 2(a)), molecules easily move between the 3-fold hollow binding sites of the substrate. The periphery of the monolayer has many branches which fluctuate significantly in shape. This is in qualitative agreement with the recent DPN experiment using 1-dodecylamine on mica [10]. As the binding strength increases (ε =6.2 kcal/mol, figure 2(b)), the irregular branches of the monolayer are missing and molecules aggregate to form a more compact pattern. The monolayer however is not perfectly compact but has some holes in it. Intriguingly, the monolayer is non-circular and looks like a hexagon. Due to the substrate anisotropy (6-fold rotational symmetry), the molecular motion on the substrate depends on its direction. The monolayer grows faster in the direction from the center to one of 6 vertices of the hexagon. Along these 6 directions, a molecule sitting at one of the hollow binding sites can move to an adjacent hollow site easily. That is, a molecule actually does not have to move on top of a gold atom in going from one hollow site to adjacent one. It can pass through the valley between two gold atoms. The direction from the center to one of 6 vertices is significantly more favored than other directions.

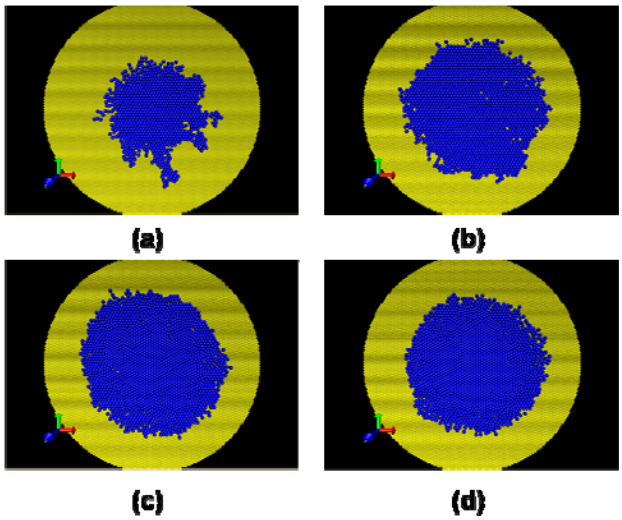

Figure 2: Final monolayer shapes for various molecule-substrate binding energies ε s. We have drawn snapshots taken at t=1.5 ns for 4 different binding energies, 3.1 kcal/mol (a), 6.2 kcal/mol (b), 12.4 kcal/mol (c), and 24.8 kcal/mol (d).

The rotational anisotropy of the substrate again manifests itself in the case of a stronger binding energy, ε =12.4

kcal/mol (figure 2(c)). A hexagonal shape of the monolayer boundary still exists. For the extremely strong molecule substrate binding (ε =24.8 kcal/mol, figure 2(d)), however, the monolayer periphery assumes a compact circular shape. Due to an extremely strong molecule-substrate binding, the molecular motion on the substrate is slow. The movement from one binding site to another takes more energy than in the previous cases. The difference in the activation energy depending on direction however becomes relatively small compared to the activation energy itself. As a result, the molecular motion becomes isotropic and the monolayer periphery becomes circular.

We quantitatively study the growth of the monolayer radius. We kept track of the number of molecules which constitute the monolayer at a given time *t*, $N(t)$. To do so, we chose molecules whose vertical distances from the substrate are within 0.45 nm. Among such molecules, we checked the intermolecular distance of every possible pair and declared the pairs with intermolecular distances below 0.95 nm as neighbors. A molecule is treated as a part of the monolayer if it is a neighbor of any molecule that forms the monolayer. Then the monolayer radius at time t, $R(t)$, is defined as $R(t)^2 = N(t)/(\pi\rho)$, where ρ is the surface density of the perfect monolayer (4.64 nm^{-2}). In Figure 3, we draw the radial growth of the monolayer for various binding energies. For all the cases, the radial growth is fast initially and then becomes slow at later times.

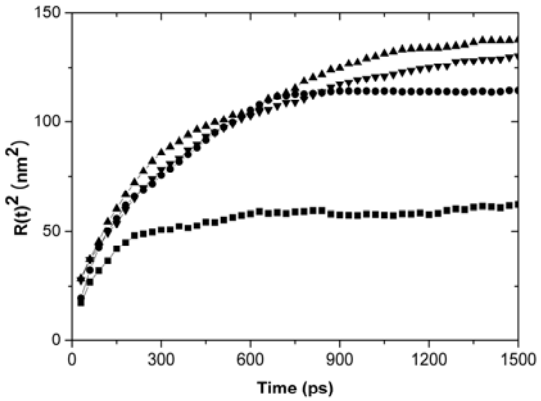

Figure 3: Radial growth of the monolayer for various molecule-substrate binding energies. We plot the radius squared, $R(t)^2$, vs. time for ε = 3.1 kcal/mol (squares), 6.2 kcal/mol (circles), 12.4 kcal/mol (upper triangles), and 24.8 kcal/mol (lower triangles).

There are two distinct phases in the monolayer growth, launching and expansion phases. During the initial launching phase, molecules flow down fast from the tip and move rapidly on the substrate. This launching phase persists until the area directly under the tip is all covered with molecules. Molecules are strongly pulled down from the tip, and the molecular spreading looks nearly inertial. This launching phase is followed by an expansion phase where the nascent monolayer around the tip expands slowly. For the expansion of the monolayer, it takes a series of pushing that needs to propagate to reach the periphery. Sometimes, many molecules move collectively toward the periphery to expand the monolayer area. The molecular motion and the monolayer growth in the expansion phase are significantly slower than in the initial launching phase.

Figure 4 shows how the final (t=1.5 ns) monolayer size depends on the molecule-substrate binding energy. The figure illustrates a turn-over behavior of the monolayer size with respect to the molecule-substrate binding energy. Up to the binding energy of 8.7 kcal/mol, increasing the binding strength raises the monolayer size. This reflects an enhanced attractive force of the substrate pulls down molecules from the tip more strongly, making the downward molecular flow from the tip faster. A further increase in the binding energy however makes the growth rate smaller. Due to a very strong binding to the substrate, molecules are now less mobile than for a smaller binding energy. The pushing of molecules from the center toward the periphery is resisted by molecules strongly sticking to the substrate.

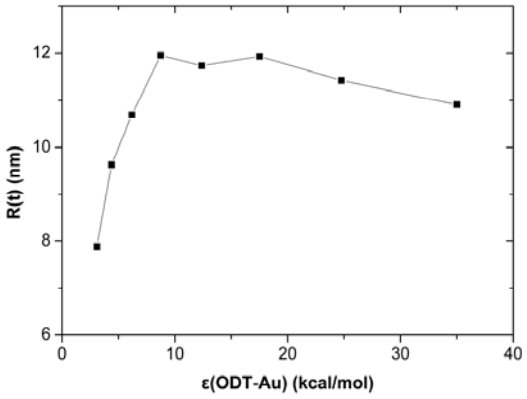

Figure 4: Final monolayer size vs. the molecule-substrate binding energy, ε. The radius $R(t)$ of the monolayer at t=1.5 ns is plotted as a function of the Lennard-Jones ε for the molecule-substrate interaction.

We also considered a cylindrical tip which contains ODT molecules in it, mimicking the "fountain-pen tip" used in DPN [11]. The radius and height of our cylindrical tip are 8.0 nm and 24.1 nm, respectively. The total number of molecules is 5602. The vertical distance from the tip end to the substrate is 1.3 nm. Figure 5 shows the final monolayer shapes for both the cylindrical tip and the hemispherical tip. Regardless of the molecule-substrate binding energy, the monolayer shape is similar for both tips. Therefore, one can expect that the qualitative conclusions obtained in this work will remain intact for different tip shapes.

NSTI-Nanotech 2008, www.nsti.org, ISBN 978-1-4200-8503-7 Vol. 1

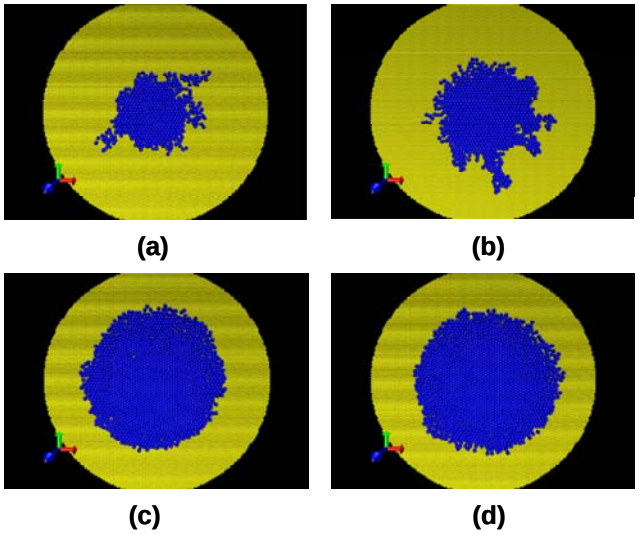

Figure 5: Dependence of the monolayer structure on the tip shape. In figures (a) and (b), we draw the final monolayer shape for the cylindrical tip and for the hemispherical tip, respectively. The molecule-substrate binding energy ε is 3.2 kcal/mol in both cases. Figures (c) and (d) show the final monolayer shapes of the cylindrical tip and hemispherical tip, respectively. In both caes, ε is 25.5 kcal/mol.

4 CONCLUSIONS

In contrast to its wide applications of dip-pen nanolithography, our understanding of the molecular mechanism of this technique and the timescale of the monolayer growth is at its infancy. We thus have performed molecular dynamics simulations to study the growth mechanism and rate, and the shape of the monolayer deposited from a nanoscale tip. Using the coarse grained molecular model which captures the essential features of alkanethiol, we have examined the monolayer growth. The pushing mechanism found in our previous study of a small sized monolayer holds for a monolayer with a diameter up to 24 nm. That is, molecules deposited from the tip push out molecules already on the substrate, and molecules pushed out in turn push other molecules nearby. When such a pushing propagates to the periphery, sometimes in a collective manner, the monolayer size grows. We have investigated how the monolayer structure is affected by the molecule-substrate binding energy. For a weak binding energy, the monolayer pattern is limited in size and has irregular branches. As the binding strength increases, the monolayer becomes compact and dense, consistent with experimental observations in dip-pen nanolithography.

We found the monolayer becomes hexagonal due to the substrate anisotropy for a moderate binding strength. An extremely strong molecule-substrate binding erases this anisotropy effect, giving a circular periphery. The monolayer growth occurs in two phases, an initial fast launching phase and a slow expansion phase. Interestingly, the speed of monolayer growth shows a turn-over behavior with respect to the increase in the binding strength. The growth speed initially increases with raising the molecular binding energy, reflecting the enhanced attraction from the substrate. A further rise in the binding energy however slows down the growth. This means that an extremely strong binding strength can make molecules immobile and block the propagation of molecular pushing toward the periphery.

We also simulated the monolayer growth by using a cylindrical tip. The monolayer does not change much in shape by changing the tip. This implies our current conclusions are quite general regardless of the tip shape.

REFERENCES

[1] C. A. Mirkin, ACS Nano 1, 79, 2007.

[2] Y. Ahn, S. Hong, and J. Jang J. Phys. Chem. B 110, 4270, 2006.

[3] M. P. Allen and D. J. Tildesley, Computer Simulation of Liquids, Clarendon Press, 1987.

[4] L. Zhang and S. Jiang, J. Chem. Phys. 117, 1804, 2002.

[5] J. Zhou, X. Lu, Y. Wang, and J. Shi, Fluid Phase Equlib. 172, 279, 2000.

[6] C. A. Alves, E. L. Smith, and M. D. Porter, J. Am. Chem. Soc. 114, 1222, 1992.

[7] L. Zhang, R. Balasundaram, S. H. Gehrke, and H. Jiang, J. Chem. Phys. 114, 6869, 2001.

[8] L. Zhang, W. A. Goddard III, and S. Jiang, J. Chem. Phys. 117, 7342, 2002.

[9] H. J. C. Berendsen, J. P. M. Postma, W. F. van Gunsteren, A. DiNola, and J. R. Haak, J. Chem. Phys. 81, 3684, 1984.

[10] P. Manandhar, J. Jang, G. C. Schatz, M. A. Ratner, and S. Hong, Phys. Rev. Lett. 90, 115505, 2003.

[11] S. Deladi, N. R. Tas, J. W. Berenschot, G. J. M. Krijnen, M. J. de Boer, J. H. de Boer, M. Peter, and M. C. Elwenspoek, Appl. Phys. Lett. 85, 5361, 2004.